Workspace and rotational capability analysis of a spatial 3-DoF parallel manipulator*

LIU Xinjun[1]**, WANG Jinsong[1], WANG Qiming[2] and LI Tiemin[1]

(1. Manufacturing Engineering Institute, Department of Precision Instruments, Tsinghua University, Beijing 100084, China; 2. National Astronomical Observatories, Chinese Academy of Sciences, Beijing 100012, China)

Received November 3, 2003; revised June 11, 2004

Abstract The analysis on the workspace and rotational capability of HANA, a spatial 3-DoF parallel manipulator, is concerned. The parallel manipulator consists of a base plate, a movable platform, and three connecting legs. The moving platform has three degrees of freedom (DoFs) which are two translations and one rotation, with respect to the base plate. The new parallel manipulator is very interesting for the reason of no singularity in the workspace, the single-DoF joint architecture and high rotational capability of the moving platform. The inverse kinematics problem is described in a closed-form, which is very useful to present the workspace geometrically. The constant-orientation and reachable workspaces for the manipulator are analyzed firstly. The index that is used to evaluate the rotational capability of the manipulator is defined and discussed in detail. Finally, the distribution of rotational capability index on the workspace is presented, which helps us know how much the index is at different point. The parallel manipulator has wide application in the fields of industrial robots, simulators, micro-motion manipulators, and parallel kinematics machines.

Keywords: parallel manipulator, singularity, rotational capability, workspace, kinematics.

In the past two decades, there have been considerable developments in the field of parallel manipulators because they can be used as industrial robots[1], simulators[2], force/torque sensors[3], micromanipulators[4,5], and parallel kinematics machine[6]. After the design concept of a manipulator with parallel kinematics was introduced by Stewart in 1965[7], especially, since the 1980s, many parallel manipulators with specified degrees of freedom (DoFs) have been developed. Most of them can be identified in the book written by Merlet[8]. Besides those, most recently, some novel parallel manipulators were proposed[9~12].

Workspace is the region where a manipulator can reach. Rotational capability is one index to evaluate whether a device is available for the task in hand or not. One of the disadvantages in parallel manipulators is its relatively small useful workspace, especially, the lower rotational capability[13], which limits their applications in the industry. The analysis of rotational capability of the output link (moving platform) in the workspace is one of the most important issues in the design and application of a parallel kinematics. Unfortunately, to the authors' knowledge, there are few reports about evaluating the rotational capability of the moving platform at one point in the workspace of a parallel manipulator. What is more, there are few parallel manipulators with high rotational capability.

HANA, a new spatial 3-DoF parallel manipulator with three non-identical chains, was proposed by Liu and Wang.[11] The movable platform has three DoFs, which are two degrees of translational freedom and one degree of rotational freedom, with respect to the base plate. The inverse kinematics problem of the parallel manipulator is given, which is basic for the analysis on the workspace and rotational capability. The workspace for the manipulator is analyzed systematically, and especially, the index to evaluate the rotational capability of the moving platform of the manipulator is defined and discussed in detail. In the manipulator, only single-DoF joints are involved in the rotational configurations, which leads to high rotational capability performance of the manipulator. The parallel manipulator studied here has wide applications in the fields of industrial robots, simulators, micro-motion manipulators, and parallel machine tools. The analysis presented in this paper can be of

* Supported by the National Natural Science Foundation of China (Grant No. 50305016)

** To whom correspondence should be addressed. E-mail: xinjunl@yahoo.com

great help in the design, application and control of such devices.

1 Description of the manipulator

The parallel manipulator was firstly proposed by Liu and Wang[11], which consists of a base plate, a movable platform, and three legs that connect the aforementioned two plates. Each connecting leg has four DoFs. Two of the three legs have identical chains, each of which consists of a planar four-bar parallelogram and three 1-DoF joints. The third one consists of a 2-DoF joint (or two 1-DoF joints) and two 1-DoF joints. A 1-DoF joint in each leg is actuated.

The manipulator, shown in Fig. 1, contains a triangular plate referred to as the output platform 14. The platform is an isosceles triangle described by its parameter r, where $O'P_i = r$ ($i = 1, 2, 3$), as shown in Fig. 2. Vertices of this platform are connected to a fixed-base plate, consisting of 3, 7 and 11, through three legs 1, 5 and 12. In this paper the three legs are called the first, second and third legs, respectively. Legs 1 and 5 have identical chains, each of which consists of a length-fixed link, a planar four-bar parallelogram, which is connected to a revolute joint 15 or 16 at the bottom end and a passive revolute joint 4 or 6 at the other. The revolute joint is then attached to an active slider 2 or 8, which is mounted on the guideway 3 or 7. The third leg 12 is very different from the former two legs. It consists of a length-fixed link which is connected to a universal joint (or two revolute joints) 13 at the bottom end and a passive revolute joint 9 at the other. The revolute joint is attached to an active slider 10, which is mounted on the guideway 11. Parameter R designates the size of the base platform, that is $OA = OB = OC = R$. The movement of the moving platform is achieved by the movement of the three sliders on the guideways.

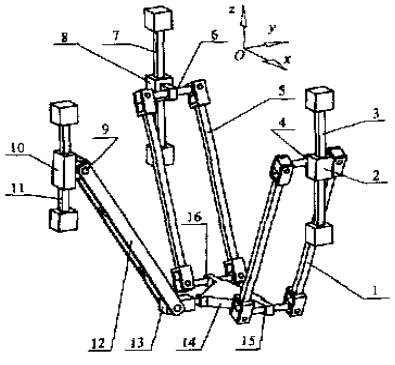

Fig. 1. The spatial 3-DoF parallel manipulator, HANA.

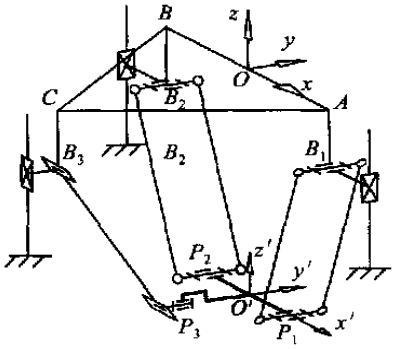

Fig. 2. Geometric parameters of HANA

According to the manipulator capability analysis presented by Liu and Wang[11], the manipulator has three DoFs, which are two translations in O-yz plane and one rotational degree of freedom about y-axis. Here, O-xyz is a fixed global reference system, which is defined in Section 2.1.

2 Basic kinematics analysis of HANA

2.1 Inverse kinematics

A kinematics model of the manipulator is developed as shown in Fig. 2. Vertices of the output platform are denoted as platform joints P_i ($i = 1, 2, 3$), and vertices of the base platform are denoted as A, B and C. A fixed global reference system $\Re$: O-xyz is located at the center of the side AB with the z-axis normal to the base plate and the x-axis directed along BA. Another reference frame, called the top frame $\Re'$: O'-$x'y'z'$, is located at the center of the side P_1P_2. The z'-axis is perpendicular to the output platform and x'-axis directed along P_2P_1. The length of link for each leg is denoted as L, where $P_iB_i = L$, $i = 1, 2, 3$. What we should note is that, in some cases, the length of the link P_3B_3 can be different from that of P_1B_1 and P_2B_2.

For the inverse kinematics analysis, the pose of the moving platform is considered known, and the position is given by the position vector $(\boldsymbol{O}')_{\Re}$ and the orientation is given by a matrix $\boldsymbol{Q}$. And there are

$$(\boldsymbol{O}')_{\Re} = (x \quad y \quad z)^{\mathrm{T}}, \tag{1}$$

where $x = 0$,

$$\boldsymbol{Q} = \begin{bmatrix} \cos\phi & 0 & \sin\phi \\ 0 & 1 & 0 \\ -\sin\phi & 0 & \cos\phi \end{bmatrix}, \tag{2}$$

where the angle ϕ is the rotational DoF of the output platform with respect to y-axis. The coordinate of the point P_i in the frame $\Re$ can be described by the vector $(\boldsymbol{p}_i)_{\Re}$ ($i = 1, 2, 3$), and

$$(\boldsymbol{p}_1)_{\mathfrak{R}} = (r \quad 0 \quad 0)^{\mathrm{T}}, \quad (\boldsymbol{p}_2)_{\mathfrak{R}} = (-r \quad 0 \quad 0)^{\mathrm{T}},$$
$$(\boldsymbol{p}_3)_{\mathfrak{R}} = (0 \quad -r \quad 0)^{\mathrm{T}}. \tag{3}$$

Vectors $(\boldsymbol{b}_i)_{\mathfrak{R}} (i=1, 2, 3)$ will be defined as the position vectors of B_i in frame $\mathfrak{R}$ and

$$(\boldsymbol{b}_1)_{\mathfrak{R}} = (R \quad 0 \quad z_1)^{\mathrm{T}}, \quad (\boldsymbol{b}_2)_{\mathfrak{R}} = (-R \quad 0 \quad z_2)^{\mathrm{T}},$$
$$(\boldsymbol{b}_3)_{\mathfrak{R}} = (0 \quad -R \quad z_3)^{\mathrm{T}}. \tag{4}$$

The vector $(\boldsymbol{p}_i)_{\mathfrak{R}} (i=1, 2, 3)$ in frame O-xyz can be written as

$$(\boldsymbol{p}_i)_{\mathfrak{R}} = \boldsymbol{Q}(\boldsymbol{p}_i)_{\mathfrak{R}} + (\boldsymbol{O}')_{\mathfrak{R}} \tag{5}$$

Then the inverse kinematics of the parallel manipulator can be solved by writing the following constraint equation

$$\| [\boldsymbol{p}_i - \boldsymbol{b}_i]_{\mathfrak{R}} \| = L, \quad i = 1, 2, 3, \tag{6}$$

which leads to

$$(r\cos\phi - R)^2 + y^2 + (z - r\sin\phi - z_1)^2 = L^2, \tag{7}$$

$$(R - r\cos\phi)^2 + y^2 + (z + r\sin\phi - z_2)^2 = L^2, \tag{8}$$

$$(y + R - r)^2 + (z - z_3)^2 = L^2. \tag{9}$$

Hence, for a given manipulator and for prescribed values of the position and orientation of the platform, the required actuator inputs can be directly computed from Eq. (6), that is

$$z_1 = \pm\sqrt{L^2 - (r\cos\phi - R)^2 - y^2} + z - r\sin\phi, \tag{10}$$

$$z_2 = \pm\sqrt{L^2 - (R - r\cos\phi)^2 - y^2} + z + r\sin\phi, \tag{11}$$

$$z_3 = \pm\sqrt{L^2 - (y - r + R)^2} + z. \tag{12}$$

From Eqs. (10), (11) and (12), we can see that there are eight inverse kinematics solutions for a given pose of the parallel manipulator. To obtain the inverse configuration as shown in Fig. 1, each one of the signs "±" in Eqs. (10) ~ (12) should be "+".

2.2 Jacobian matrices

Eqs. (7), (8) and (9) can be differentiated with respect to time to obtain the velocity equations, which leads to

$$(z - r\sin\phi - z_1)\dot{z}_1 = y\dot{y} + (z - r\sin\phi - z_1)\dot{z} + [(z_1 - z)r\cos\phi + Rr\sin\phi]\dot{\phi}, \tag{13}$$

$$(z + r\sin\phi - z_2)\dot{z}_2 = y\dot{y} + (z + r\sin\phi - z_2)\dot{z} + [(z - z_2)r\cos\phi + Rr\sin\phi]\dot{\phi}, \tag{14}$$

$$(z - z_3)\dot{z}_3 = (y - r + R)\dot{y} + (z - z_3)\dot{z}. \tag{15}$$

Rearranging Eqs. (13) ~ (15) leads to an equation of the form

$$\boldsymbol{A}\dot{\rho} = \boldsymbol{B}\dot{\boldsymbol{p}}, \tag{16}$$

where $\dot{\boldsymbol{p}}$ is the vector of output velocities defined as

$$\dot{\boldsymbol{p}} = (\dot{y} \quad \dot{z} \quad \dot{\phi})^{\mathrm{T}}, \tag{17}$$

and $\dot{\rho}$ is the vector of input velocities defined as

$$\dot{\rho} = (\dot{z}_1 \quad \dot{z}_2 \quad \dot{z}_3)^{\mathrm{T}}. \tag{18}$$

Matrices $\boldsymbol{A}$ and $\boldsymbol{B}$ are, respectively, the 3×3 inverse and forward Jacobian matrices of the manipulator and can be expressed as

$$\boldsymbol{A} = \begin{bmatrix} z - r\sin\phi - z_1 & 0 & 0 \\ 0 & z + r\sin\phi - z_2 & 0 \\ 0 & 0 & z - z_3 \end{bmatrix}, \tag{19}$$

$$\boldsymbol{B} = \begin{bmatrix} y & z - r\sin\phi - z_1 & r(z_1 - z)\cos\phi + Rr\sin\phi \\ y & z + r\sin\phi - z_2 & r(z - z_2)\cos\phi + Rr\sin\phi \\ y - r + R & z - z_3 & 0 \end{bmatrix}. \tag{20}$$

Jacobian matrices $\boldsymbol{A}$ and $\boldsymbol{B}$ will be used to analyze the singularity.

3 Workspace analysis

3.1 Constant-orientation workspace

The constant-orientation workspace is defined as the region that can be reached by the reference point on the moving platform when the orientation of moving platform is kept constant. In this paper, the workspace will be discussed firstly.

Eqs. (7) ~ (9) can be rewritten as

$$y^2 + [z - (r\sin\phi + z_1)]^2 = L^2 - (R - r\cos\phi)^2, \tag{21}$$

$$y^2 + [z - (z_2 - r\sin\phi)]^2 = L^2 - (R - r\cos\phi)^2, \tag{22}$$

$$[y - (r - R)]^2 + (z - z_3)^2 = L^2, \tag{23}$$

from which we can see that if z_1, z_2, z_3 and ϕ are specified, Eqs. (21) ~ (23) represent three circles in the plane O-yz. For the first leg, the circle is centered at $(0, r\sin\phi + z_1)$ and the radius is $\sqrt{L^2 - (R - r\cos\phi)^2}$. For the second leg, the circle is centered at $(0, z_2 - r\sin\phi)$ and the radius is $\sqrt{L^2 - (R - r\cos\phi)^2}$. And for the third one, $(r - R, z_3)$ and L are the center and radius of the circle, respectively. Indeed, if the mechanical interference is neglected, the boundary of the workspace for each leg is attained whenever at least one of the actuators reaches one of its limits. If we assume that ϕ is specified and the range of motion of the actuators

is given by

$$z_1,\ z_2,\ z_3 \in [z_{\min}, z_{\max}], \tag{24}$$

the workspace for each leg is the enveloping face of innumerable circles. The constant-orientation workspace of the parallel manipulator is the intersection of the three enveloping faces.

3.2 Reachable workspace

The reachable workspace is known as the region that can be reached by the reference point with at least one orientation. Firstly, let us investigate the intersection of two enveloping faces expressed by Eqs. (21) and (22). That is, if ϕ is given and z_1 and z_2 are specified by Eq. (24) whether the intersection between the constant-orientation workspaces of the first and second legs exists. Based on Eqs. (21) and (22), we assume that there is intersection for $\phi \in [0, 90^\circ]$, then boundaries of the orientation workspace intersection should be $y^2+[z-(r\sin\phi+z_{\min})]^2=L^2-(R-r\cos\phi)^2$ and $y^2+[z-(z_{\max}-r\sin\phi)]^2=L^2-(R-r\cos\phi)^2$. In this case, the relationship between $r\sin\phi+z_{\min}$ and $z_{\max}-r\sin\phi$ must be

$$z_{\max}-r\sin\phi > r\sin\phi+z_{\min}, \tag{25}$$

that is

$$\sin\phi < (z_{\max}-z_{\min})/2r, \tag{26}$$

which is the condition to the possible intersection of the orientation workspaces for the first and second legs when $0 \leqslant \phi \leqslant 90^\circ$. Similarly, if $\phi \in [-90^\circ, 0)$ and there is intersection, circles $y^2+[z-(r\sin\phi+z_{\max})]^2=L^2-(R-r\cos\phi)^2$ and $y^2+[z-(z_{\min}-r\sin\phi)]^2=L^2-(R-r\cos\phi)^2$ should be the boundaries. Then, the condition for the possible intersection of the orientation workspaces will be $z_{\max}+r\sin\phi > z_{\min}-r\sin\phi$, which is the same as Eq. (26).

From above analysis, one can see that Eq. (26) is actually the condition for the possible intersection of orientation workspaces for the first and second legs. The reachable workspace for the first and second legs is the combination of all such orientation workspaces of the two legs, which is denoted as Ω_{R12}. And the reachable workspace for the third leg, which is the region given by Eq. (23), is denoted as Ω_{R3}. The reachable workspace of the parallel manipulator can be expressed as

$$\Omega_R = \Omega_{R12} \cap \Omega_{R3}. \tag{27}$$

Generally, in most industrial applications, we just consider basically the orientation workspace with $\phi=0$, which is denoted as Ω_{OW_0}. Based on such workspace, some performances, e.g. the rotational capability of the device, can be investigated ulteriorly. Usually, the boundaries of the workspace can be given by

$$C_a: y^2+(z-z_{\max})^2 = L^2-(R-r)^2, \tag{28}$$

$$C_b: y^2+(z-z_{\min})^2 = L^2-(R-r)^2, \tag{29}$$

$$C_c: [y-(r-R)]^2+(z-z_{\min})^2 = L^2, \tag{30}$$

$$C_d: [y-(r-R)]^2+(z-z_{\max})^2 = L^2. \tag{31}$$

In this paper, the workspace outside the orientation workspace with $\phi=0$ is assumed unusable. The rotational capability analysis in the following sections is also simply based on the orientation workspace with $\phi=0$.

4 Rotational capability analysis

Rotational capability analysis is to evaluate how much the rotational DoF could reach. We know that among the rotational configurations there are singularities, especially the second kind of singularity. Therefore, we should firstly investigate the singularity. According to the classification of the singularities pertaining to parallel manipulators[26], the second kind of singularity arises when $\boldsymbol{B}$ becomes singular but $\boldsymbol{A}$ is invertible, i.e. when

$$\det(\boldsymbol{A}) \neq 0 \quad \text{and} \quad \det(\boldsymbol{B}) = 0. \tag{32}$$

In such a configuration, the output link is locally movable even when all the actuated joints are locked, and the output link cannot resist one or more forces or moments even when all actuators are locked.

Generally, this kind of singularity occurs in the configurations related to the rotational DoF[9]. The rotational DoF related actuation is that the first and second legs provide. Therefore, the research of the second kind of singularity just involves the configurations of the first and second legs.

Assuming that the first leg P_1B_1 is in the moving platform plane, that is

$$r(z_1-z)\cos\phi+Rr\sin\phi=0, \tag{33a}$$

which leads to

$$\tan\phi=(z_1-z)/R. \tag{33b}$$

If the manipulator is in a singular configuration, there must be

$$|\boldsymbol{B}| = [r(z-z_2)\cos\phi+Rr\sin\phi][y(z-z_3)-(y-r+R)(z-r\sin\phi-z_1)] = 0. \tag{34}$$

The condition to Eq. (34) is

$$r(z-z_2)\cos\phi + Rr\sin\phi = 0, \quad (35)$$

which gives the information that the second leg is also in the moving platform plane. Then the condition to the second kind of singularity of the manipulator is that the first and second legs are in the moving platform plane, simultaneously. This singularity will make a negative influence on the rotational capability.

According to the kinematics of the spatial 3-DoF parallel manipulator, the rotational DoF of the manipulator is the rotation of the moving platform with respect to y-axis as shown in Fig. 1. Considering the structure of the manipulator, one can see that the first and second legs are in the same status for the rotational DoF. This reminds us that, for a given position (y, z) in the workspace, if ϕ satisfies Eq. (10), it must satisfy Eq. (11), which can be easily found out from Eqs. (10) and (11). Therefore, to investigate the rotational capability of the rotational DoF, one of the first and second legs can be considered firstly. From Eqs. (3) and (5), the position vector $(\boldsymbol{p}_1)_{\Re}$ can be written as

$$(\boldsymbol{p}_1)_{\Re} = (r\cos\phi \quad y \quad z - r\sin\phi)^{\mathrm{T}}. \quad (36)$$

Let $x_{p1} = r\cos\phi$, $y_{p1} = y$ and $z_{p1} = z - r\sin\phi$, Eq. (21) can be rewritten as

$$(x_{p1} - R)^2 + y_{p1}^2 + (z_{p1} - z_1)^2 = L^2, \quad (37)$$

which stands for a spherical surface centered at $(R, 0, z_1)$, and the radius is L. If z_1 is specified and the workspace point (y, z) is given, Eq. (37) represents a circle centered at point (R, y, z_1), and the radius is $\sqrt{L^2 - y^2}$. The equation can be rewritten as

$$(x_{p1} - R)^2 + (z_{p1} - z_1)^2 = L^2 - y^2, \quad (38)$$

which is located on the plane paralleling to O-xz plane given by y. If z_1 is specified as $z_1 \in [z_{\min}, z_{\max}]$, Eq. (38) represents some circles with the same radius $\sqrt{L^2 - y^2}$. Considering the manipulator studied here, for a given position (y, z) of the moving platform, the locus of point P_1 is the subset of a circle of radius r. The equation can be written as

$$x_{p1}^2 + (z_{p1} - z)^2 = r^2, \quad (39)$$

which is located at the plane paralleling to O-xz plane, defined by y. What is more, we can see that two circles defined by Eqs. (38) and (39) are located on the same plane. When (y, z) and z_1 are specified, the intersecting point (x_{p1}, z_{p1}) of the two circles can be obtained.

Eq. (38) minus Eq. (39) produces

$$z_{p1} = fx_{p1} + g, \quad (40)$$

where $g = (L^2 - y^2 - r^2 + z^2 - z_1^2 - R^2)/2(z - z_1)$ and $f = R/(z - z_1)$. Substituting Eq. (40) into Eq. (38) leads to

$$A' x_{p1}^2 + B' x_{p1} + C' = 0, \quad (41)$$

where $A' = 1 + f^2$, $B' = 2f(g - z)$ and $C' = (g - z)^2 - r^2$. Then there is

$$x_{p1} = \frac{-B' \pm \sqrt{B'^2 - 4A'C'}}{2A'}. \quad (42)$$

z_{p1} can also be obtained by substituting Eq. (42) into Eq. (40). From Eqs. (40) and (42), we can see that there are two intersecting points. If z_1 changes between $z_{\min}$ and $z_{\max}$, all such intersecting points can be reached, the set of which is actually an (or two) arc(s), part(s) of the circle given by Eq. (39). The arc(s) is(are) then the possible locus of point P_1 for the first leg for a given parallel manipulator. Every point on the arc(s) represents the possible configuration of the moving platform at a given point in the workspace.

As mentioned above, a given value ϕ that satisfies Eq. (10) can undoubtedly satisfy Eq. (11). Even though, one can notice that, from Eqs. (10) and (11), if z_1 obtained from Eq. (10) for a specified orientation ϕ is within $[z_{\min}, z_{\max}]$, one cannot be sure that z_2 in Eq. (11) is also available between $z_{\min}$ and $z_{\max}$. This means that not every point on the aforementioned arc(s) corresponds to an available orientation of the parallel manipulator. Then the question in the face for this case is how the orientation of the manipulator could be, and how to define the rotational capability of the parallel manipulator. From Eqs. (10) and (11), one can also find out that if z_1 is within $[z_{\min}, z_{\max}]$ for a given ϕ, z_2 can also be within $[z_{\min}, z_{\max}]$ for the orientation $-\phi$ but not ϕ. This can help us to know which point on the arc is the real locus of point P_1 for a given parallel manipulator. That is if $\phi_{\max} > 0$ is the maximum orientation that the manipulator can reach at a specified point (y, z) in the workspace Ω_{OW_0}, the available orientation of the manipulator must be $[-\phi_{\max}, \phi_{\max}]$, which is symmetric with respect to the axis x''. In this paper, x'' is defined as the axis that is located at point (y, z) and is parallel to x-axis. This result will be discussed in detail based on an example in the next section. The index ζ to evaluate the rotational capability of the moving platform at the given position (y, z) is then defined as

$$\zeta = 2\phi_{\max}. \quad (43)$$

What we should notice is that, possibly, these con-

figurations for the orientation $[-\phi_{max}, \phi_{max}]$ include that of singularities, which will separate the arc into two manipulator-inaccessible ones. Actually, the rotational capability of a real manipulator device can only be valued by one of the two arcs. For the manipulator as shown in Fig. 1, only the second kind of singularity will occur in a usable workspace of a manipulator. What should be considered here is the singularity of the first and second legs B_1P_1 and B_2P_2. This singularity occurs when the first and second legs are in the moving platform plane, simultaneously. Actually, it is not easy to reach such singularity for the parallel manipulator. If the actuation is given reasonably, there is no singularity in the workspace for such a parallel manipulator. The detailed presentation of the rotational capability will be discussed by an example in the following section.

5 An example

As an example of application of the analysis for the new parallel manipulator presented in this paper, the workspace and rotational capability of a spatial 3-DoF parallel manipulator with $r=3.0$, $R=12.0$ and $L=15.0$ are considered here.

If the actuated motion is specified as

$$z_1, z_2, z_3 \in [-3.0, 3.0], \tag{44}$$

the second kind of singularity will occur only in the case that B_1P_1, P_1P_2 and P_2B_2 are completely extended or folded. In such a configuration, inputs for the first and second legs should be long enough. For example, at point $(y=0.0, z=-12.0)$, when B_1P_1, P_1P_2 and P_2B_2 are completely extended the inputs should be $z_1=-25.42$ and $z_2=1.42$, respectively, which can be obtained from Eqs. (10) and (11). This indicates that z_1 is beyond the input limit given in Eq. (44), i.e. there is no input condition to the singular configuration at this point. For the given manipulator, because $L-r=R$, the completely folded singular configuration occurs only when the first and second legs are both parallel to x axis. In the configuration, the orientation of the manipulator will be 180° or -180°. Therefore, it is not easy for the parallel manipulator to reach the second kind of singularity. For the given parallel manipulator, the moving platform cannot reach the orientation as much as 180° or -180°, which will be shown in the following analysis.

In order to find the singular configurations, we can mirror the first and second legs P_1B_1 and P_2B_2 and the moving platform into the plane O-xz, and the mirrors are $P_1'B_1$, $P_2'B_2$ and $P_1'P_2'$, respectively, as shown in Fig. 3. For a specified point (y, z) in the workspace, the first and second inputs for the second kind of singularity can be expressed as

$$\begin{cases} z_1 = z - \sqrt{(B_2P_2'+r)^2-R^2}, \\ z_2 = z + \sqrt{(B_2P_2'+r)^2-R^2}, \end{cases} \tag{45}$$

for the case of completely extended configuration, and

$$\begin{cases} z_1 = z - \sqrt{(B_2P_2'-r)^2-R^2}, \\ z_2 = z + \sqrt{(B_2P_2'-r)^2-R^2}, \end{cases} \quad B_2P_2'-r \geqslant R \tag{46}$$

for the case of completely folded configuration, especially, if $B_2P_2'-r<R$, there is no condition to the folded singularity. In the two equations, $B_2P_2'=\sqrt{L^2-y^2}$. If z_1 and z_2 in any one of the above two equations are both within $[z_{min}, z_{max}]$, there is the second kind of singularity at the point (y, z); otherwise, there is no such singularity.

According to the analysis of the workspace in Section 3.2, the reachable workspace Ω_R of the example can be obtained as the shade region in Fig. 4 (a). The area of the workspace is 32.7980, which can be obtained easily with the help of a commercial software, AutoCAD R14. Fig. 4 (b) shows the orientation workspace Ω_{OW_0}, in which the boundaries of the workspace given by Eqs. (28) ~ (31) are illustrated. The area is 31.7521, which is little less than that of Ω_R. The following analysis on the rotational capability is based on this workspace.

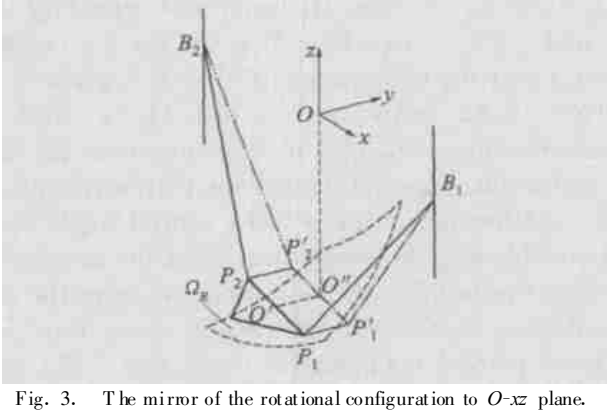

Fig. 3. The mirror of the rotational configuration to O-xz plane.

As an example to present the rotational capability index, the reference point O' on the moving platform is specified as $c(y_c=-2.0, z_c=-12.0)$ in the workspace Ω_{OW_0}. The circle described by Eq. (39)

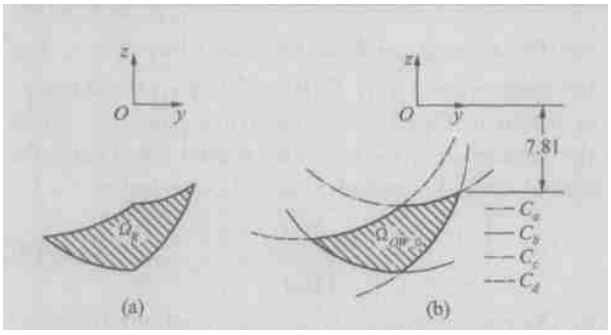

Fig. 4. Workspace of the manipulator for the example in Section 5. (a) The reachable workspace, (b) the orientation-workspace with $\phi = 0$.

is denoted as ν centered at point c in the plane O_y-$x_y y_y$, which is parallel to plane O-xy and there is $OO_y = y_c$, as illustrated in Fig. 5. The region, which is the locus of point P_1 on the first leg given by Eq. (38) when $z_1 \in [-3.0, 3.0]$, in the plane O_y-$x_y y_y$ is also shown in Fig. 5. The part of circle ν that is embodied in the region is arc ab. Points a and b are actually the intersecting points between circle ν and the circle given by Eq. (38) when $z_1 = z_{\min}$. Arc ab is then the locus of point P_1 when the moving platform is locked at point c and the second leg is not considered. It is obvious that the angle $\angle bcx''$ is no less than $\angle acx''$, and the mirror of point a about x'' axis is point a', which is on the arc ab. As analyzed in the previous section, if z_1 is within $[z_{\min}, z_{\max}]$ for a given orientation ϕ, z_2 can also be within $[z_{\min}, z_{\max}]$ for the orientation $-\phi$. Extending it to this example, if point P_1 is located at any point of arc aa', both z_1 and z_2 can be within $[-3.0, 3.0]$. Otherwise, if point P_1 is located at arc ba', z_2 will not be available between -3.0 and 3.0. The central angle of arc aa' is then the rotational capability index, and $\zeta = 2\angle x''ca = 89.65^\circ$ at the point c, which indicates that the tilting angle of the moving platform can be $\pm 44.82^\circ$ and $\phi_{\max} = \angle x''ca = 44.82^\circ$. Fig. 6 (a) shows the simulation of configurations for the first and second legs and the moving platform in plane O-xz. As mentioned above, the central angle contains possibly singular configurations of the manipulator. And the singular configurations separate the arc aa' into two manipulator-inaccessible ones. But, for the given parallel manipulator, from Eqs. (45) and (46), one can see that if the second kind of singularity occurs in the workspace, one of the inputs z_1 and z_2 for the first and second legs must be no more than -7.81. It is in conflict with the given input limit $[-3.0, 3.0]$. Then there is no singularity in the workspace for the given parallel manipulator.

Generally, the rotational capability of the manipulator studied here can be expressed as

$$\zeta = 2\left|\tan^{-1}(z_{p1}/x_{p1})\right|, \qquad (47)$$

in which z_{p1} and x_{p1} can be obtained from Eqs. (40) and (42) when $z_1 = z_{\min}$ for the case $z_{p1} < z_c$, and $z_1 = z_{\max}$ if $z_{p1} > z_c$, especially, $\zeta = 0$ if $z_{p1} = z_c$.

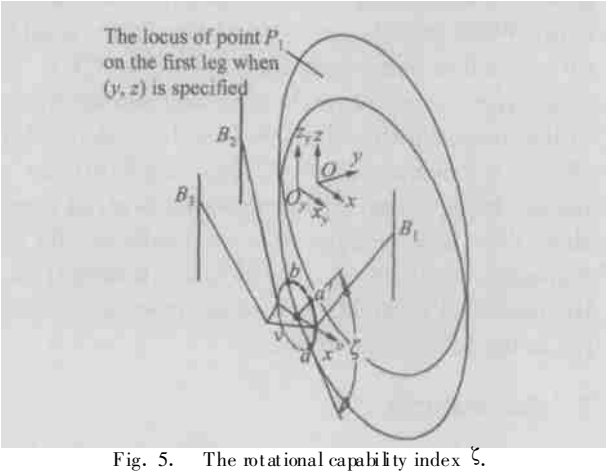

Fig. 5. The rotational capability index ζ.

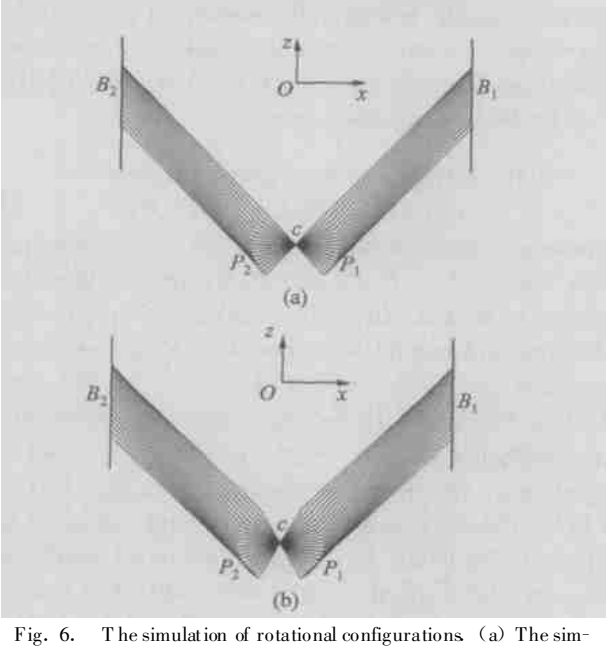

Fig. 6. The simulation of rotational configurations. (a) The simulation for the normal case; (b) the simulation for the adjusted case.

Based on above analysis results, we can obtain all rotational capability values of the manipulator for points in the workspace Ω_{OW_0}. Fig. 7 represents the distribution of the rotational capability index on the workspace, which shows that

(i) The distribution is symmetric with respect to z-axis. In other words, the rotational capability at point (y, z) is identical to that at point $(-y, z)$;

(ii) On boundary curves of the workspace defined by the first and second legs, i.e. the curves described by Eqs. (28) and (29), the rotational capability of the manipulator is zero. This is obvious because the first and second inputs reach their limit at these points. More than that, at the point near the curves the rotational capability is very low;

(iii) In the region $z \in [-12.2, -10.3]$, the index ζ is very high $\zeta \geqslant 90^\circ$. The maximum value of ζ can reach 139.2°.

From the obtained results, the rotational output of the proposed parallel manipulator is only related to the first and second legs. The rotational capability will depend on the first and second inputs and the position of point O' in the workspace, and for a given point, it just depends on the two inputs. Therefore, in the process of design for a device based on HANA, one can increase the input limits $z_{\min}$ and $z_{\max}$ of the first and second legs to improve the rotational capability of the device. For example, if inputs for the two legs are changed to $[-4.0, 4.0]$, the rotational capability of the manipulator at point c ($y_c = -2.0$, $z_c = -12.0$) will be increased to $\zeta = 117.92^\circ$. Fig. 6 (b) shows the simulation of configurations of this case.

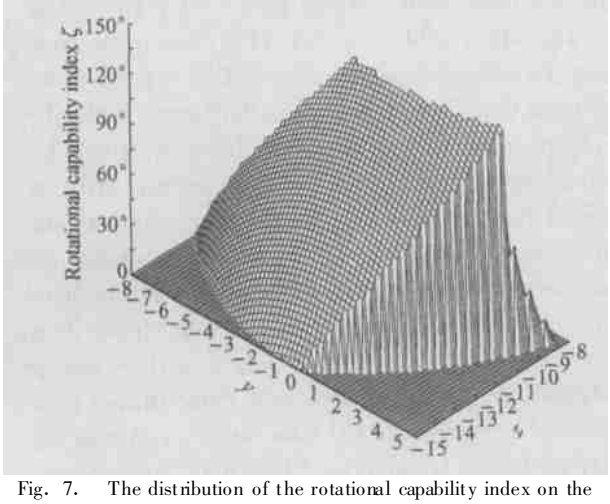

Fig. 7. The distribution of the rotational capability index on the workspace.

6 Conclusions

In this paper, the workspace and rotational capability of a spatial 3-DoF parallel manipulator, HANA, are analyzed. HANA has three DoFs, which are two degrees of translational freedom and one degree of rotational freedom. The advantages of the parallel manipulator are: (a) only single-DoF joints are used; (b) combining spatial translational and rotational DoFs in a spatial 3-DoF parallel manipulator; (c) high rotational capability of the rotational DoF. The workspace, reachable and constant-orientation workspaces, of the manipulator is analyzed. The rotational capability index of the manipulator is defined to evaluate the rotational capability in the workspace. The results show that there is no singularity in the workspace; and the rotational capability could be very high with a reasonable design. The parallel manipulator has wide applications in the fields of industrial robots, simulators, micro-motion manipulators, and parallel machine tools.

References

1 Cleary, K. et al. Kinematics analysis of a novel 6-DOF parallel manipulator. In: Proc. IEEE International Conference on Robotics and Automation, TX, USA, 1993, 708.
2 Salcudean, S. E. et al. A six degree-of-freedom, hydraulic, one person motion simulator. In: Proc. IEEE International Conference on Robotics and Automation, CA, USA, 1994, 2437.
3 Kerr, D. R. Analysis, properties and design of stewart platform transducer. Trans. ASME, J. Mech. Transm. Automn. Des., 1989, (111): 25.
4 Reboulet, C. et al. Hybrid control of a 6-DOF in-parallel actuated micro-manipulator mounted on a scara robot. In: Proceedings of the International Symposium on Robotics and Manufacturing: Research, Education and Applications, Burnaby Canada, 1990, 293.
5 Liu, X. J. et al. On the design of 6-DoF parallel micro-motion manipulators. In: Proceedings of IEEE/ RSJ International Conference on Intelligent Robots and Systems, Hawaii, USA, 2001, 343.
6 Valenti, M. Machine tools get smarter. ASME Mechanical Engineering, 1995, 17: 70.
7 Stewart, D. A platform with six degrees of freedom. Proc. Inst. Mech. Eng., 1965, 180: 371.
8 Merlet, J. P. Parallel Robots. Netherlands: Kluwer Academic Publishers, 2000.
9 Liu, X. J. et al. On the analysis of a new spatial three degrees of freedom parallel manipulator. IEEE Transactions on Robotics and Automation, 2001, 17: 959.
10 Kong, X. et al. Kinematics and singularity analysis of a novel type of 3-CRR 3-DOF translational parallel manipulator. The International Journal of Robotics Research, 2002, 21: 791.
11 Liu X. J. and Wang, J. Some new parallel mechanisms containing the planar four-bar parallelogram. International Journal of Robotics Research, 2003, 22: 717.
12 Fang, Y. et al. Structure synthesis of a class of 4-DoF and 5-DoF parallel manipulators with identical limb structures. International Journal of Robotics Research, 2002, 21: 799.
13 Tonshoff, H. K. et al. A systematic comparison of parallel kinematics. In: Parallel Kinematics Machines. London: Springer-Verlag, 1999, 295.
14 Daniali, H. R. M. et al. Singularity analysis of a general class of planar parallel manipulators. In: Proceedings of IEEE International Conference on Robotics and Automation, Nagoya, Japan, 1995, 1547.